Applied Catalysis B: Environmental 111–112 (2012) 254–263

Contents lists available at SciVerse ScienceDirect

Applied Catalysis B: Environmental

journal homepage: www.elsevier.com/locate/apcatb

Heterogeneous Fenton using ceria based catalysts: effects of the calcination temperature in the process efficiency

André F. Rossi, Nuno Amaral-Silva, Rui C. Martins, Rosa M. Quinta-Ferreira *

CIEPQPF, Centro de Investigação em Engenharia dos Processos Químicos e Produtos da Floresta, GERSE, Group on Environment, Reaction and Separation Engineering, Department of Chemical Engineering, Faculty of Sciences and Technology, University of Coimbra, Pólo II – Rua Sílvio Lima, 3030-790 Coimbra, Portugal

ARTICLE INFO

Article history:
Received 29 July 2011
Received in revised form
24 September 2011
Accepted 4 October 2011
Available online 8 October 2011

Keywords:
Heterogeneous Fenton's process
Catalyst characterization
Environment protection
Phenolic acids
Toxicity

ABSTRACT

The need of more efficient solid catalysts for the heterogeneous slurry Fenton process led many investigators to research new compounds activities. Ceria based iron catalysts have proved their good performance enhancing the removal of organic compounds, reducing toxicity and improving biodegradability in the depuration of phenolic wastewaters. This work evaluates the calcination temperature (300 °C, 600 °C and 1000 °C) during the preparation of the catalysts—co-precipitation of the precursors salts, while the same previously optimized conditions were adopted (pH 3.0, 1.0 g L^{-1} of Fe–Ce–O 70/30 as the catalyst, [H_2O_2] = 244 mM and 120 min of room temperature reaction) to treat a simulated wastewater comprising 0.1 g L^{-1} of each of the six common phenolic acids found in Olive Mills wastewaters. The three obtained solids were characterized regarding superficial area, average pore diameter, FT-IR and XRD. Catalysts calcinated at 300 °C, 600 °C and 1000 °C presented superficial areas of 188, 86 and 2 m^2/g, respectively, and their average pore diameter are 66, 87 and 151 Å, correspondingly. As showed in the XRD, the increase of the calcination temperature promotes the crystallinity of the obtained solid—higher amount of prominent peaks, meaning that the catalysts have different states of valence for iron (Fe^{2+} or Fe^{3+}) and ceria (Ce^{2+} to Ce^{4+}), what would explain their singular behaviours during the reaction. As expected, the solids with higher superficial areas had better performances in every aspect: more COD, TOC and phenolic acids removal, pointing the lowest calcination temperature as leading to a more efficient solid to enhance hydrogen peroxidation, involving, however, more metal leaching. The higher the calcination temperature is, the more oxidized the solid will become because the calcination occurs without atmospheric control and so the oxygen contained in the air will interfere on the valence of iron ions at the solid's surface. This means that a solid calcinated at a higher temperature will have increased Fe^{3+} content and, as one can find in the literature, Fe^{2+} is more effective than Fe^{3+} at hydrogen peroxidation, explaining the better efficiency of the catalyst calcinated at the lowest temperature. Toxicological and biodegradability studies were still performed and showed enhancement in all cases.

1. Introduction

People's needs, which once were simple, have greatly increased through ages. The meaning of the word "evolution" sometimes only encompasses the fulfilling of those needs, without noticing that this thirst becomes, in a certain way, an enemy of life itself. New products are being elaborated every day and, as the number of different substances that happen to be often in our daily activities increases, another necessity—not rarely forgotten, raises: to treat these compounds before disposal.

Wastewater treatment, sooner than having practical application, is a scientific study that needs plenty of effort concerning the environment's welfare—giving priority to remediate the streams of discharge that will reach water courses in order not to damage them.

Fenton's oxidative reaction was discovered in the early 1890s. Basic mechanisms for the reaction were proposed only almost 40 years later [1,2]. Even today there is still a polemic argumentation over which pathways Fenton's reagent may have to oxidize compounds. Although the mechanisms are not well enlightened, this reaction became a very powerful method of wastewater treatment as an advanced oxidation process that has the advantage of occurring at mild conditions. Before reaching industrial scale, procedure studying and efficiency evaluation are fundamental so the system can be optimized to economically fit the meanings to an end. Homogeneous Fenton's process was firstly investigated and literature can be found in the remediation of different kinds of effluents: olive mill wastewaters [3–6], winery [7,8], pesticides [9]. Besides

* Corresponding author. Tel.: +351 239798723; fax: +351 239798703.
E-mail address: rosaqf@eq.uc.pt (R.M. Quinta-Ferreira).

0926-3373/$ – see front matter © 2011 Elsevier B.V. All rights reserved.
doi:10.1016/j.apcatb.2011.10.006

specific studies, there are also reviews and overviews that one may consult to obtain overall knowledge comprising several aspects of the reaction separately, such as the works of Neyens and Bayens [10] and Bautista et al. [11].

Although different conclusions are taken according the effluent being handled and the objective of the work (that may focus economic viability, remediation of the wastewater, biodegradability enhancement, color removal, between others), one will find that the most crucial problem laying at the homogeneous Fenton's process is the formation of ferrous sludge—another waste that will require a separation step and further treatment. Avoiding this unwanted drawback, heterogeneous Fenton's process is raising as the natural development of the former procedure. Instead of adding iron ion (Fe^{2+} or Fe^{3+}) precursors, such as the commonly used $FeSO_4{\cdot}7H_2O$, $FeCl_3$ or $Fe(NO_3)_3{\cdot}9H_2O$, the heterogeneous method lays that the iron catalyst will be present but not dissolved, being thus impregnated at the surface of a solid. Activated carbon [12], polymer encapsulation [13], silica [14], clays [15,16], metallic oxides [17,18] have been part of the vast investigation regarding iron supports. Our group of investigation has recently screened heterogeneous catalysts based on cerium, manganese and iron oxides, finding promising results with the former. Different molar proportions of iron-to-cerium were then tested and had their efficiencies evaluated, being possible to observe that the most active cerium based iron oxide has the proportion Fe/Ce of 70/30 [19]. Cerium has proved its good efficiency in different advanced oxidation processes such as catalytic wet oxidation [20,21], and ozonation [22].

Still aiming the optimization of the process, the present work encompasses another parameter in the preparation of the catalyst above-mentioned (Fe–Ce–O 70/30) that was not yet studied: the calcination temperature. Experiments results allowed the catalyst's efficiency assessment while treating a simulated olive mill wastewater comprising six of the most common phenolic acids found in this effluent.

2. Experimental

2.1. Catalyst preparation and characterization

Between the catalysts previously studied by our research group, Fe–Ce–O was highlighted due to its higher efficiency [19]. This work used three different Fe–Ce–O 70/30 catalysts prepared at the laboratory by co-precipitation of an aqueous solution of the former metallic salts: iron nitrate (*Riedel-de-Häen*) and cerium nitrate (*Riedel-de-Häen*) containing the desired molar proportion, 70/30 (other ratios were tested before but this specific one showed higher efficiency). Precipitation is stimulated by an increase on the pH by the addition of 200 mL of a 3 M solution of sodium hydroxide. The precipitate is filtrated, washed with 2.5 L of distilled water, dried at 105 °C for 2 h, powdered by manual milling and then calcinated during 3 h, as the procedure proposed by Silva et al. [20]. As the present study has the intention of determining the best calcination temperature regarding removals of TOC, COD and TPh, as well as toxicity annulment and biodegradability enhancement of the resulting catalyst, three temperatures were chosen: 300, 600 and 1000 °C—which will name the prepared solids as C_{300}, C_{600} and C_{1000}, respectively, to facilitate comprehension and further discussion.

In order to characterize these catalysts, they were submitted to the following analysis: (i) Brunauer–Emmet–Teller surface area (S_{BET}) determined by an accelerated surface area and porosimetry analyzer *ASAP 2000 V2.04* (*Micrometrics*) with nitrogen at −196 °C, (ii) X-ray diffraction (XRD) through a conventional and low angle *X-ray diffractometer Philips model X-Pert*, (iii) mercury porosimetry for porosimetry and pore size distribution assessment at a *Poresizer 9320* (*Micrometrics*), (iv) gas (helium) picnometry in an *AccuPyc 1330 V2.01* (*Micromeritics*), (v) laser dispersion to particle size assessment (*Malvern Mastersizer 2000 V5.60 - Malvern Instruments*) and (vi) scanning electron microscopy (SEM) with a *JEOL JSM-5310*.

Table 1
Characteristics of the synthetic effluent comprising six phenolic acids at 0.1 g L^{-1} each.

COD (mg O_2 L^{-1})	1000 ± 80	EC_{20} (%)	4.5 ± 2
BOD_5 (mg O_2 L^{-1})	279 ± 56	EC_{50} (%)	32.2 ± 2
BOD_5/COD	0.28	Toxicity (%)	67.0 ± 8
TOC (ppm)	418 ± 8	Biodegradability (%)	2.0 ± 8
pH	3.3 ± 0.05		

2.2. Synthetic effluent stock solution confection

The preparation of the phenolic solution consists in the addition of 0.1 g of each of the acids (3-4-5-trimethoxybenzoic acid, 4-hydroxybenzoic acid, protocatechuic acid, syringic acid, vanillic acid and veratric acid) to 1 L of distilled water. To overcome the low solubility of these compounds in water and ensure their dissolution, the solution is submitted to ultrasounds (*Crest ultrasounds equipment*) during 15 min. Afterwards, the pH of the solution is adjusted to 3.0—with $H_2SO_4{\cdot}2N$ or NaOH 0.3 M, in order to obey previously obtained conclusions that affirm this pH value leads to the best efficiency [19]. With this methodology, a solution with the characteristics mentioned in Table 1 was subsequently used.

As shown in Table 1, the simulated wastewater has high toxicity (this parameter is explained in the next section) and low biodegradability (proven by respirometric tests and LUMIStox analysis), being inappropriate for biological depuration [20]—which emphasizes the necessity of chemical treatment.

2.3. The Fenton's process itself

Reactions were carried out in 500 mL capacity glass reactors magnetically stirred in which 300 mL of the synthetic effluent stock solution were poured just before the addition of the required amount of catalyst. Then pH monitoring is started with a *Crison MicropH 2000* probe inserted inside the reactor and continuously adjusted to 3.0—with H_2SO_4 0.2 N or NaOH 0.3 M. The reaction only begins with the slow addition of the desired volume of H_2O_2. At certain time intervals, samples were withdrawn by direct pippeting from the reactor to a vacuum filtration unit (funnel, kitassato and air pump) using a 0.45 μm pore diameter quantitative filter paper to remove the solid catalyst from the liquid phase. Immediately after filtration, NaOH 3 M is added to the filtrated sample in order to raise the pH above 9.5, stopping, this way, the reaction by quenching the remaining H_2O_2 since it interferes with some of the analytical techniques. Samples were then named and stored in the refrigerator at approximately 4 °C until being forwarded to analysis.

2.4. Analytical techniques—synthetic effluent and treated samples

Total organic carbon (TOC) analyses were conducted in a *Shimadzu 5000 Analyser* coupled with an auto-sampler *ASI - 5000A*. Total phenolic content (TPh) was assessed colourimetrically by the Folin-Ciocalteau procedure [23,24] with a *T60 U PG instruments* spectrophotometer for absorbance measurement. Standard Method 5220D was utilized to determine the chemical oxygen demand (*COD*) [25], in which *WTW CR 3000* thermoreactor and a *WTW MPM 3000 photometer* were used. Biochemical oxygen demand in 5 days (BOD_5) was measured by the method proposed on the Standard Methods, being the inoculums obtained from

Table 2
Catalysts characterization.

	Catalyst		
	C_{300}	C_{600}	C_{1000}
Calcination temperature (°C)	300	600	1000
B.E.T. surface area (m^2/g)	188	86	2
Pore diameter (Å)	66	87	151
Single point total pore volume (cm^3/g)	0.311	0.189	0.008
Average density (g/cm^3)	3.99	5.41	5.72

garden soil [26]. Toxicity assessment was evaluated through the light inhibition of the marine bacteria *Vibrio fischeri* after 15 min of incubation on the presence of the samples—being this analysis essential to infer about the ecosystems harm that may occur by the discharge into natural water courses of the potentially toxic wastewaters. A commercial analyzer LUMIStox (*Dr. Lange*), which operates according to the standard DIN/EN/ISO 11348, was used to carry out this procedure—consisting in the determination of the wastewater effective concentration that causes the inhibition of 20% (EC_{20}) and 50% (EC_{50}) of the bacteria by measuring the intensity of its light glowing before and after 15 min of contact with the sample. Also, a liquid static-static (LSS) respirometer was used to evaluate biodegradability and toxicity through respirometric techniques. Biodegradability assessment was made upon the oxygen uptake rate (OUR) of activated sludge (obtained from a winery wastewater treatment plant with volatile suspended solids between 3000 and 4000 mg/L) while consuming a completely biodegradable compound ($OUR_{acetic\ acid\ I}$) and compared with the OUR of the same bacteria population being fed by the analyzed sample (OUR_{sample}), according to Eq. (1). Still using the same parameter, toxicity was measured by comparing the OUR while consuming acetic acid ($OUR_{acetic\ acid\ II}$) of the bacteria after being exposed to the potentially toxic sample, as in Eq. (2).

$$\text{Biodegradability}_{\%} = \left(\frac{OUR_{sample}}{OUR_{acetic\ acid\ I}}\right) \times 100 \quad (1)$$

$$\text{Toxicity}_{\%} = \left(\frac{OUR_{acetic\ acid\ I} - OUR_{acetic\ acid\ II}}{OUR_{acetic\ acid\ I}}\right) \times 100 \quad (2)$$

Oxidation/reduction potential (ORP) and pH monitoring were carried out with a *Crison micropH 2000*. A spectrometer *Perkin-Elmer 3300* was used to quantify the iron leaching to the liquid phase.

In order to assess sample's hydrogen peroxide content, *QUANTOFIX® Peroxide 25* test strips were employed. Once the concentration in the bulk is much higher than the measuring kit's sensitiveness, samples are diluted to 1:1000, 1:2000, 1:5000 and 1:10,000. To each diluted solution, a strip is used to measure peroxide content. The given value is then multiplied to the corresponding dilution factor—the highest and the lowest results are discarded while the others have its media calculated. The use of four dilutions has the intention of diminishing errors (found out to be close to 15% through peroxide stock solution concentration determination by the strips) and improving accuracy, since the result is given though color comparison between the used strip and a pattern—a sensitive analysis that depends on the manipulator's decision. This procedure requires to be made without any delay due to the fast and spontaneous hydrogen peroxide decomposition.

3. Results and discussion

3.1. Fresh catalyst characterization

Even though the composition of the three catalysts is the same, the change of the calcination temperature imposes singular properties to the resulting solid and these can be seen in Table 2.

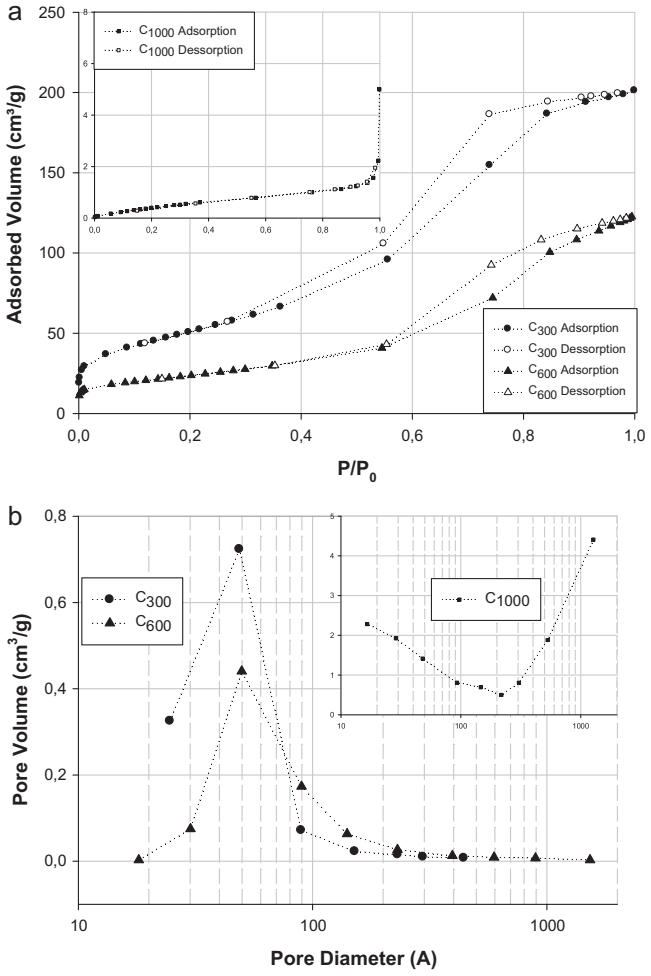

Fig. 1. (a) Gas adsorption isotherms (adsorbed volume versus relative pressure). Inlet: C_{1000} curves, which have a lower scale. (b) Pore size versus pore volume graphs. Inlet: curve for C_{1000}, which has a greater scale.

Fig. 1a illustrates fresh catalysts' gas adsorption isotherms. According to Figueiredo and Ribeiro [27]: (i) C_{300} and C_{600} isotherms are correspondent to standard isotherms type IV, characterized by the hysteresis phenomenon and the presence of an elbow; a solid that presents this kind of isotherm usually has mesopores. (ii) C_{1000} isotherm corresponds to a standard isotherm type II, meaning that this solid either has no pores or has macropores. Numerical values were already presented in Table 2.

Fig. 1b shows the relation between pore volume and diameter. The curves indicate that C_{300} and C_{600} have most of their pores within diameters smaller than 100 Å, while C_{1000} has much greater ones. These data interpretations are ensured by the single point total pore volume, which decreases with the raise of the calcination temperature, and the opposite happens regarding the average density. Through Table 2, one can conclude that C_{300}'s pores have a smaller diameter and large volume. The same happens to C_{600}, but for C_{1000} the pore diameters are wide their total pore volume is very small. This also explains the great differences between the surface areas: small amount of great sized pores leads to lower superficial area (C_{1000}) while a higher number of deeper pores (despite of the reduced diameter) "enlarge" the available surface (C_{300} and C_{600}).

In order to evaluate another solid's aspect that might correlate its structure and catalytic behaviour, X-ray diffraction characterization analysis was performed. While C_{300} shows a completely amorphous pattern without any crystallinity, C_{600} has an increase in both and C_{1000} is the opposite, exhibiting strong peaks,

Table 3
Used catalysts characterization.

	Catalyst		
	Used C_{300}	Used C_{600}	Used C_{1000}
Calcination temperature (°C)	300	600	1000
B.E.T. surface area (m^2/g)	175	128	5
Pore diameter (Å)	69	71	91
Single point total pore volume (cm^3/g)	0.299	0.227	0.011

indicating that a higher calcination temperature leads to a more crystalline solid.

Cerium oxides present a quite important property during the calcination process. CeO_2 are capable of interacting with other metal oxides changing the metal valence state in the composite. The strong affinity and interaction between CeO_2 and Mn_2O_3 were discussed by Imamura et al. [28]. When these structures are in contact at temperatures over 150 °C, Mn^{2+} species begins to appear. We believe that the same process might occur when iron oxides are in contact with cerium oxide, explaining the reducing of Fe^{3+} (iron nitrate, the precursor) to Fe^{2+} (present in the catalyst). We also believe that this interaction might happen while the Fenton reaction occurs: as the iron begins to be oxidized, the cerium (which is in the same solid) might exchange electrons and enhance the catalyst overall activity.

3.2. Used catalyst characterization

After being used at Fenton's process, all catalysts were dried inside an oven at 105 °C and analyzed again to evaluate its properties and check for any changes. The results disposed in Table 3 will be showed along this section and commented until the end of it.

Fig. 2a illustrates used catalysts' gas adsorption isotherms. To the Used C_{300} and Used C_{600} isotherms are given the same classification (type IV: hysteresis and elbow, indications of mesopores). Only minor changes exist between used catalysts and the fresh ones. Yet former catalysts' isotherms remained almost unchanged, Used C_{1000}' continues presenting a type II isotherm but with the hysteresis phenomenon type H3, classifying the solid as a non-rigid aggregate of particles in plate form, originating cleft-shaped pores.

Comparing Used C_{300} and C_{300}, one may notice that pore diameter has slightly increased while single point total volume and B.E.T. area decreased—the opposite of what happened to the other solids after reaction. This fact can be explained by the change on the calcination temperature: higher values generate denser and more resistant solids, which will be confirmed by leaching tests, showed and commented in Section 3.4.3. Fig. 2b shows the pore distribution for the used catalysts, where one can see that there are no significant changes.

All catalysts (fresh and used) have had its image at three different scales taken—namely, 350×, 2000× and 5000× by SEM. The following Sections 3.2.1–3.2.3 will be used to show those images and include a brief discussion about them.

3.2.1. In focus: Fe–Ce–O 70/30 catalyst baked at 300 °C

It is not hard to notice the "structure loss" over the reaction comparing pictures of fresh and used C_{300}—Fig. 3. On the fresh images (Fig. 3a), the aggregates are bigger and have more "grainy attachments" while the used catalyst's surface (Fig. 3b) seems flat and with just a few small structures attached onto the aggregates.

3.2.2. In focus: Fe–Ce–O 70/30 catalyst baked at 600 °C

On C_{600}'s images, one can see that the fresh catalyst (Fig. 4a1) is not as homogeneous as the used (Fig. 4b1). Although this indicates that the catalyst is broken into smaller pieces due to the reaction agitation, the higher magnitude pictures (Fig. 4a2 against b2 and a3 against b3) comparison shows that a considerable part of the grainy structures attached to the aggregates is still there.

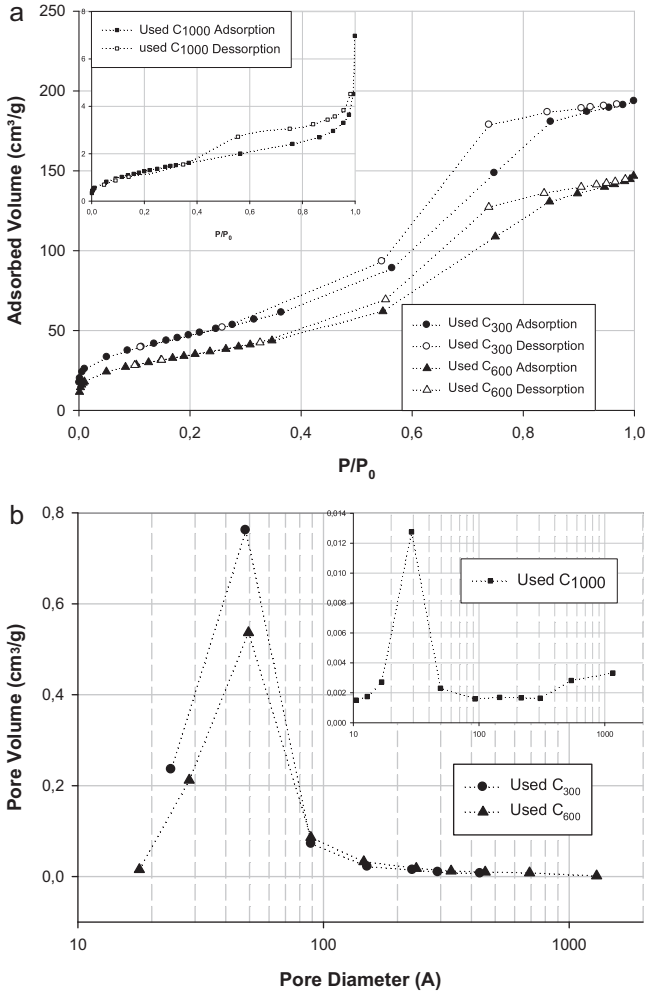

Fig. 2. (a) Gas adsorption isotherms (adsorbed volume versus relative pressure) of used catalysts. Inlet: Used C_{1000} curves, which have a lower scale. (b) Pore size versus pore volume graphs for the used catalysts. Inlet: curve for Used C_{1000}, which has a lower scale.

3.2.3. In focus: Fe–Ce–O 70/30 catalyst baked at 1000 °C

At last, C_{1000}'s illustrations (Fig. 5) reveal that the catalyst calcinated at the highest temperature is the one that remains with less significant structural changes. On a naked eye comparison, the aggregate's sizes for the fresh and used solids (Fig. 5a and b) seem closer and also the grainy surface aspect is kept.

3.3. Preliminary results

As our investigation group has worked with these kind of wastewater for a long time, plenty of experience has been acquired and optimal reaction parameters are already established, such as pH 3.0, $[H_2O_2] = 244$ mM and [Fe–Ce–O 70/30] = 1.0 g L^{-1}. Other tests were useful to ensure that: (i) for the present catalysts at these conditions, the chemical regime is applied (negligible mass transfer resistances), (ii) hydrogen peroxide alone cannot significantly oxidize the compounds (without the addition of catalyst), (iii) the catalyst just by itself removed negligible organic matter by adsorption (without hydrogen peroxide addition) [19].

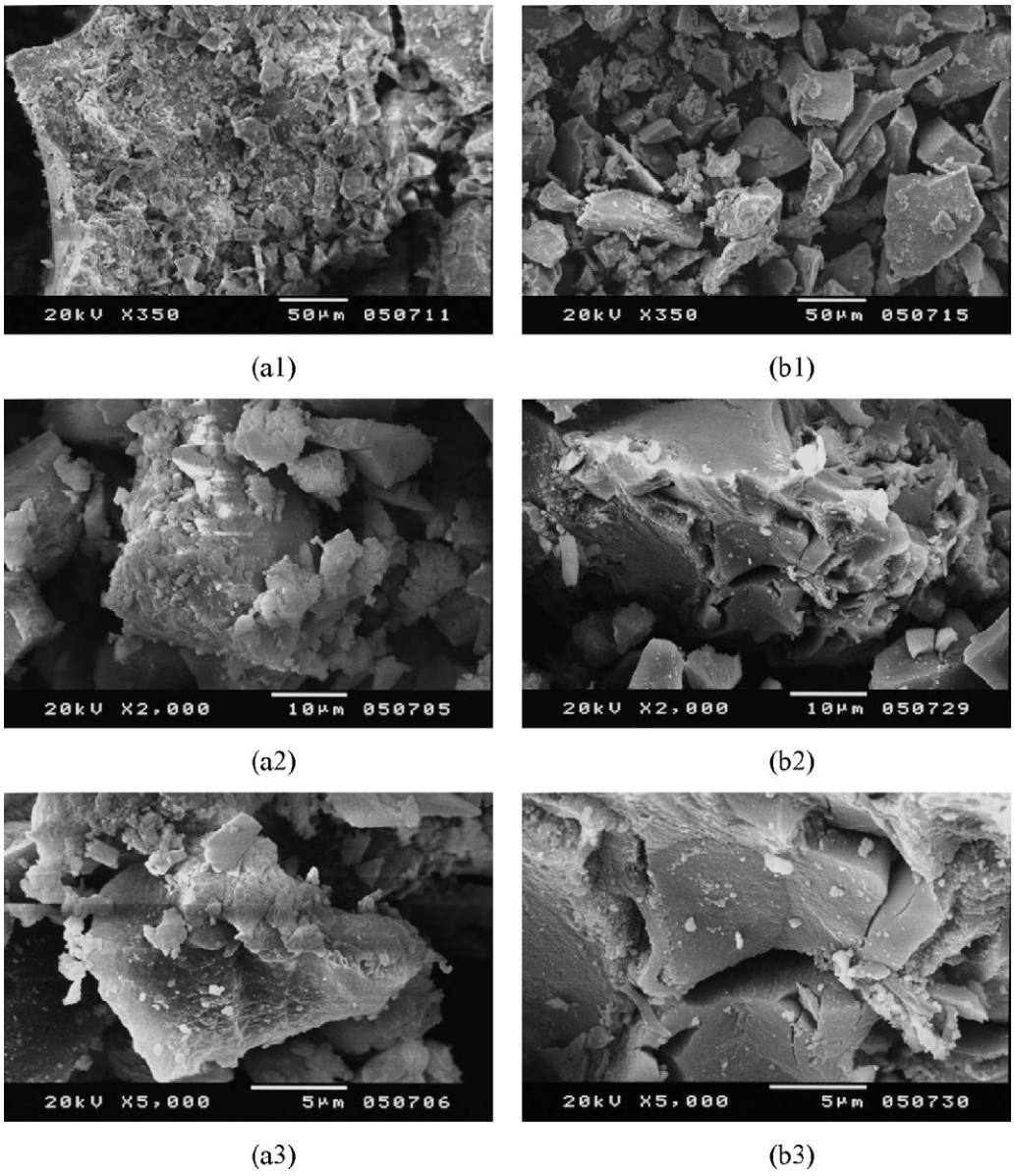

Fig. 3. SEM images showing several magnifications of fresh (a) and used (b) Fe–Ce–O calcinated at 300 °C.

3.4. Influence of the calcination temperature

Next Sections 3.4.1–3.4.3 are reserved to discuss each catalyst's experiment, featuring Fenton's process efficiency assessment in every considered aspect.

3.4.1. Organic charge depletion

As mentioned before, the synthetic effluent is composed by a mixture of six phenolic acids, with each one contributing for the increase on the TPh. It is already well known that Fenton's oxidation can easily break these aromatic bonds and this was once more observed in this work's results (Fig. 6), where C_{300} and C_{600} completely depleted these compounds. The reaction rate of phenolic destruction is high at the beginning of all experiments (over 70% of the final removal is achieved in less than 20 min) and decays along the reaction probably due to the rapid concentration decrease and the formation of refractory phenolic by-products. As opposed to the other catalysts, C_{1000} was the only one that could not entirely remove phenolic content (only approximately 70% after 2 h), pointing this solid's activity as low. C_{1000}'s low activity was also observed regarding COD removal (Fig. 7). Its final depletion reached merely half of the one obtained by C_{600} (21% and 39%, respectively). The best result was attained by C_{300}, 49%. Again, one can notice that the reaction rate decreases along time. This can be probably related to the intermediate compounds created during the experiment that become harder to oxidize as the reaction occurs, besides the fact of the arise of some refractory substances.

COD has a link with TOC and, therefore, their removals are meant to have some resemblances. Usually, TOC is removed after COD depletion, meaning that the effluent's organic substances are oxidized (COD removal), breaking molecules in smaller pieces until the limit, CO_2 and H_2O, when mineralization takes part (TOC removal). This can easily be noticed by analyzing Figs. 7 and 8. The first one shows the gradual reduction of COD, although in different levels, attained by the three catalysts. However, as shown in the second graph, when it comes to the C_{1000} related curve, negligible TOC reduction is observed—meaning that even though COD was reduced, no mineralization occurred, indicating that the reaction goes on toward oxidation but cannot get rid of small and more oxidized molecules to produce CO_2. Again, the best results

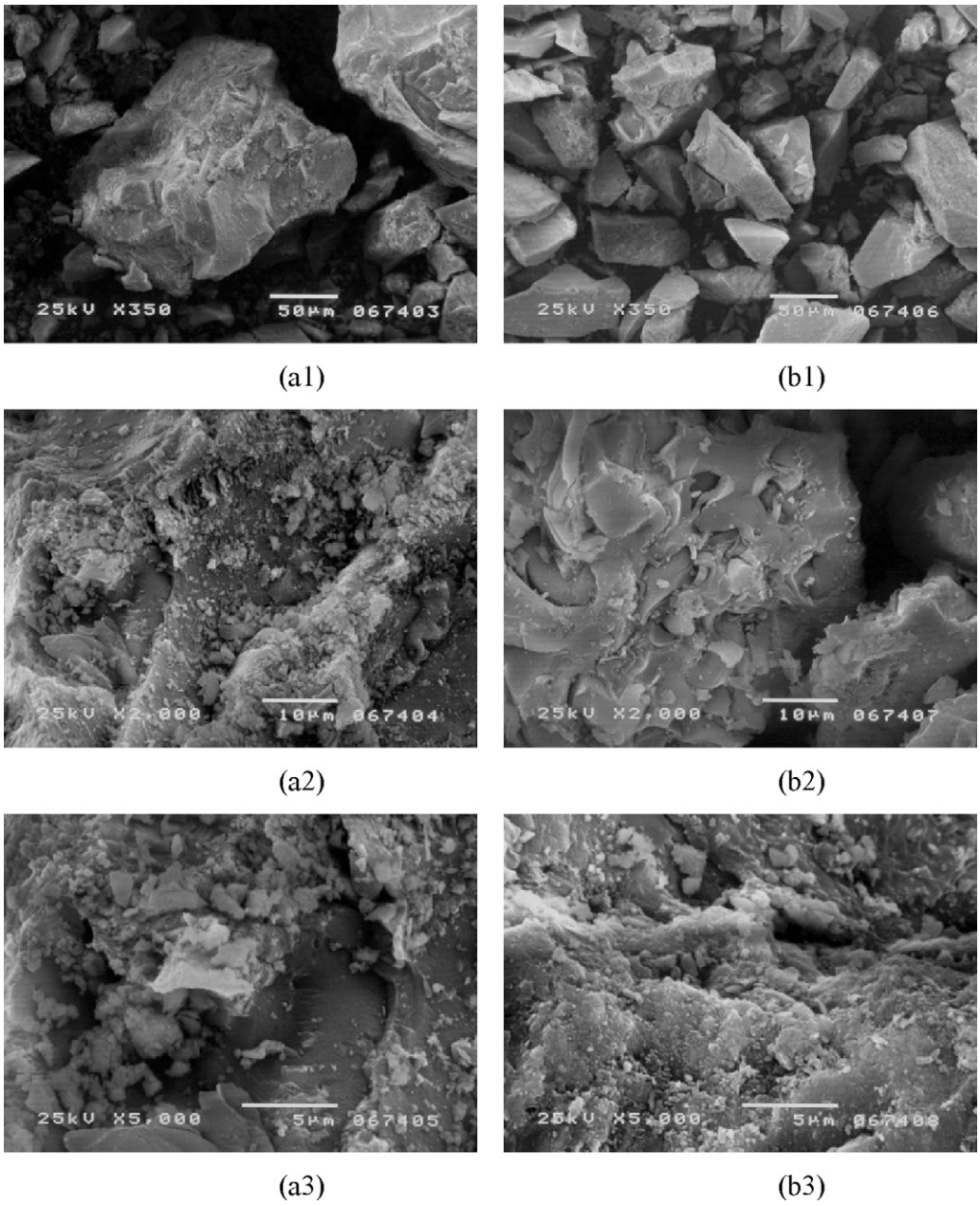

Fig. 4. SEM images showing several magnifications of fresh (a) and used (b) Fe–Ce–O calcinated at 600 °C.

for these removals were C_{300}'s, which are much higher than the others.

3.4.2. Biodegradability and toxicity assessment

As previous sections results showed, the organic load removal was not sufficient for the effluent to be directly disposed—therefore, further treatment is required. Being biological plants the most recommended, biodegradability enhancement and toxicity annulment gain great importance since phenolic wastewaters are hardly consumable by microorganisms due to its high toxicity and low biodegradability.

Although all catalysts were able to completely degrade the phenolic content, each of them presented different values of degradation by bacteria—biological oxygen demand in five days (BOD_5), meaning that not only the phenols are poisonous, but so the reaction intermediate compounds are.

As yet Fenton's reaction mechanisms are not fully traced, it is impossible to determine which molecules are harmful and which are not. Therefore, regarding final judgment the most important sample in each experiment is its last point—at the end of the 2 h reaction, because this treatment was optimized to this time. An important note is that one cannot ensure that from the beginning to the end of the reaction, the biodegradability or toxicity marches its way only increasing or decreasing. That depends on the compounds generated and eliminated by oxidation and yet is not possible to follow the bulk's (effluent) composition that closely.

BOD_5 is the primal and most reliable analysis, since toxicity through respirometry and LUMIStox sometimes creates confusion in the results discussion and affirmative conclusions are harder to be taken; besides, BOD_5 represents biodegradability examinations when the sample keeps in contact with a population of bacteria during five days—much longer than the 15 min of LUMIStox or the couple of hours that respirometry usually takes, analyzing, this way,

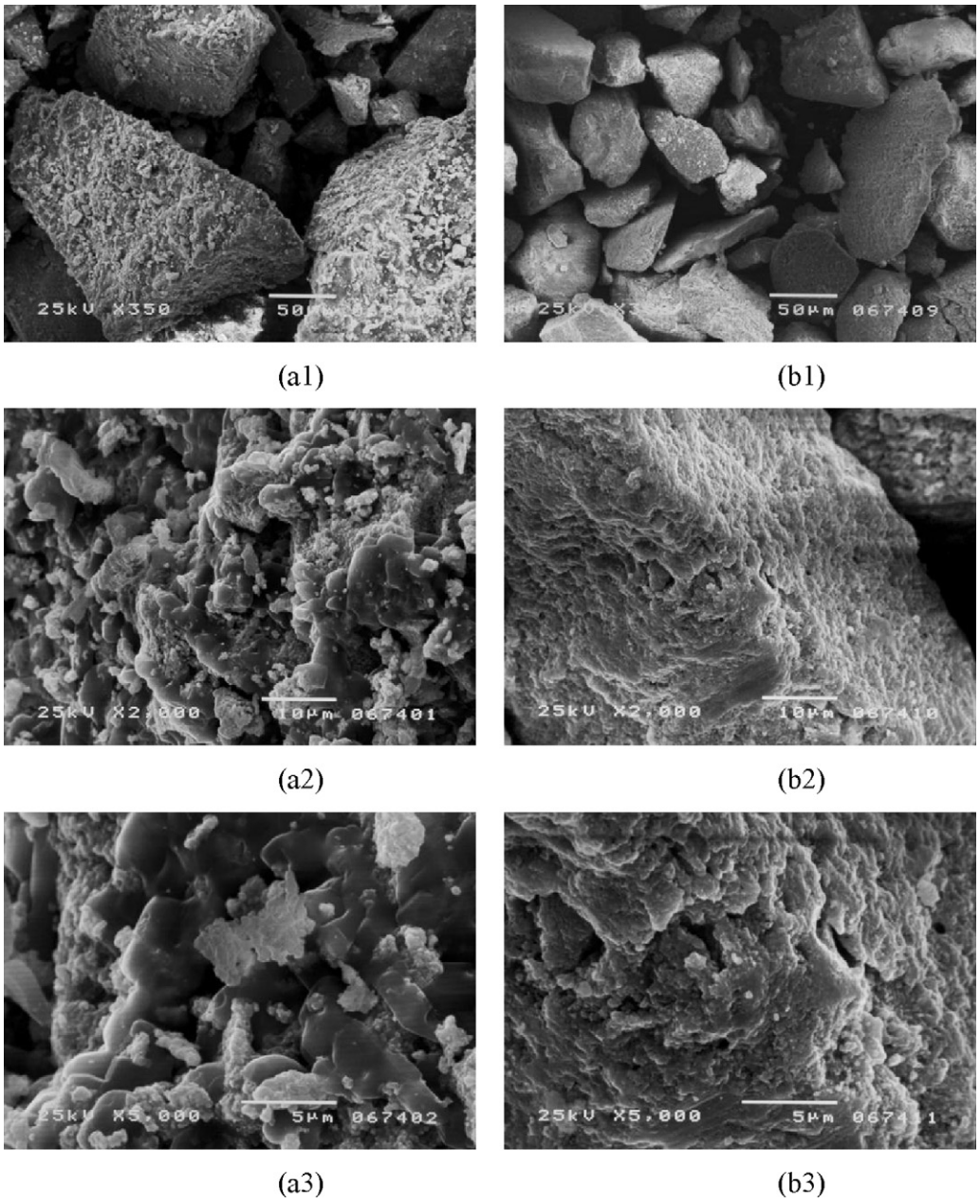

Fig. 5. SEM images showing several magnifications of fresh (a) and used (b) Fe–Ce–O calcinated at 1000 °C.

not just the immediate impact but giving also time for the bacteria to recover from their exposition to a new media. This data set is presented in Table 4 along with the respective COD values and the ratio BOD_5/COD, which represents the fraction of oxygen that can be oxidized biologically. The analysis of these data shows that the higher was the temperature that the catalysts had been exposed, the lesser was the toxicity removal after the experiments. C_{300} enhanced the BOD_5/COD ratio from 0.30 to 0.76. C_{600} was also able to elevate this value to 0.55 but, on the other hand, C_{1000} made the samples even harder to be oxidized by the microorganisms than the raw effluent, because toxic compounds may have been generated without being further degraded.

Table 4
Biological oxygen demand after 5 days (BOD_5) compared with chemical oxygen demand (COD) along with the biological/chemical oxygen demand ratio.

Raw effluent		Treated effluent—2 h of reaction			
		Catalyst	BOD_5 (mg O_2 L^{-1})	COD (mg O_2 L^{-1})	BOD_5/COD
BOD_5 (mg O_2 L^{-1})	279	C_{300}	372	489	0.76
COD (mg O_2 L^{-1})	930	C_{600}	349	630	0.55
BOD_5/COD	0.30	C_{1000}	0	790	0.00

LUMIStox values, in percentage, are displayed in Fig. 9a (EC_{20}) and Fig. 9b (EC_{50}). As discussed before, the raw effluent, by itself, presents a certain value of toxicity. A solution containing 4.5% of it is able to inhibit 20% of the bacteria *V. fischeri*, while a concentration of 32.2% is required to inhibit 50%—that is the start line for all catalysts.

Regarding C_{300}, one can see that the required amount of sample to restrain 20% of the bacteria rises from 4.5% to 12.4% in 1 h and to 62.1% in 2 h of reaction, meaning that the toxicity has been depleted during the experiment. Most likely, the concentration of the sample required to be in solution to inhibit 50% of the bacteria is higher (as in this example). This way, because of the two non-calculated

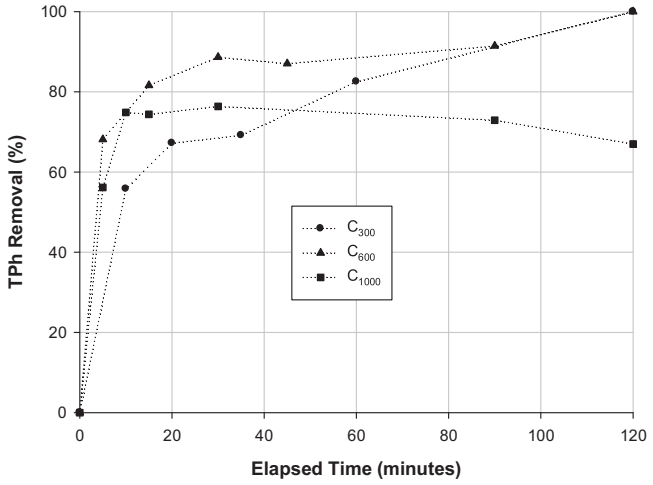

Fig. 6. Total phenolic content removal (%) curves along the experiments.

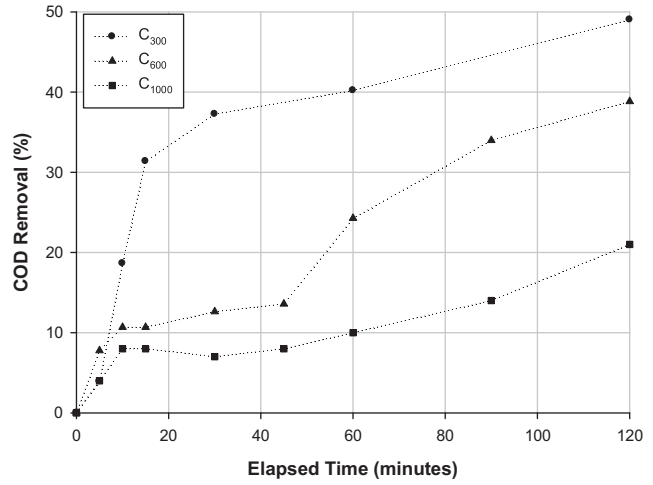

Fig. 7. Chemical oxygen demand removal (%) curves along the experiments.

values (N.C.) of EC_{50} related to C_{300} (60 and 120 min), we can say that not even the pure sample would interfere sufficiently to inhibit 50% of the bacteria—meaning that this catalyst was able to reduce the toxicity significantly.

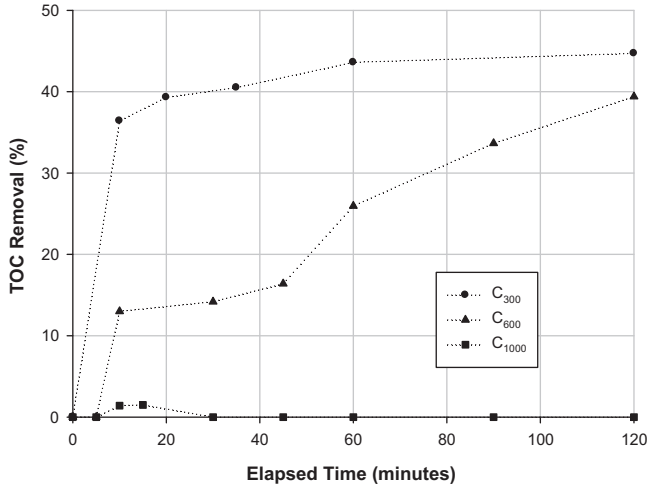

Fig. 8. Total organic carbon removal (%) curves along the experiments.

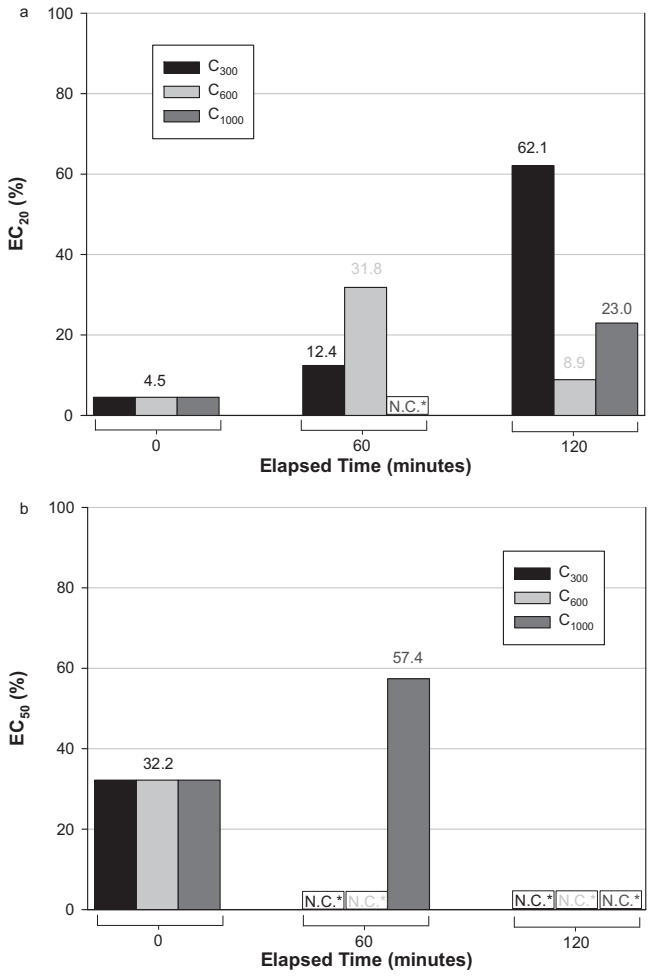

Fig. 9. (a) Percentage EC_{20} (%) vertical bar plot along the experiments. *N.C.: non-calculated value. (b) Percentage EC_{50} (%) vertical bar plot along the experiments. *N.C.: non-calculated value.

At the first hour of reaction, C_{600} presented a good result, having elevated EC_{20} from 4.5% to 31.8% and a non-calculated value of EC_{50} that could be still explained as above. But, as the reaction continues for another hour, both values of EC_{20} and EC_{50} are non-calculated and, this time, there are two possible explanations to what could be happening: (i) either the sample is so toxic that even the slightest concentration would be able to inhibit 50% of the bacteria, or (ii) the sample is not toxic at all and not even the pure sample would be able to inhibit 20% of the bacteria.

C_{1000} results present a different perspective for the first hour of reaction: while EC_{50} rises from 32.2% to 57.4%, EC_{20} becomes non-calculated. This N.C. value might be justified by the fact that the sample is still sufficiently toxic to inhibit 20% of the bacteria even at very low concentrations. This toxicity would be then reduced during the last hour of reaction, once EC_{20} reaches a value of 23% and EC_{50} becomes non-calculated. Now, it can be compared to the C_{300}'s middle reaction time value. Thus, C_{300} seems to be the most effective catalyst facing eco-toxicity reduction. Once again, the exquisite Fenton's mechanisms for each catalyst do not allow behaviour expectations for EC_{20} and EC_{50} patterns due to different intermediate compounds generation.

Respirometry analysis (data shown in Table 5) confirms and concludes this work biological assessment: higher calcination temperatures generate less efficient solids to act as Fenton catalysts regarding further biological treatment. While C_{300} was able to completely deplete toxicity (from 67% to 0) and greatly improve

Table 5
Toxicity and biodegradability values acquired trough respirometry.

Raw effluent		Treated effluent—2 h of reaction		
		Catalyst	Toxicity	Biodegradability
Toxicity	67%	C_{300}	0	70%
Biodegradability	2%	C_{600}	7%	18%
		C_{1000}	10%	4%

biodegradability (from 2% to 70%), other catalysts were not able to completely destroy toxic compounds (toxicity remains at 7% for C_{600} and 10% for C_{1000}) and their contribution to biodegradability enrichment is not as significant (18% for C_{600} and only 4% in the case of C_{1000}).

3.4.3. Catalyst stability and reaction heterogeneity

Biodegradability enhancement, toxicity annulment, COD, TOC and TPh removals are not the only factors that one may take into account while selecting a catalyst. A solid that has no resistance to maintain its active sites on their own spots is not proper for long-term industrial applications because it would have to be replaced over and over again, generating unnecessary waste of financial resources. Each catalyst of this work had its experiment's final sample analyzed to assess the amount of iron present in solution. This allows the evaluation of the iron leaching and the stability of the catalyst, presented in Fig. 10.

Reuse experiments of the same catalyst (Fe–Ce–O) were already carried out by our research group [19]. This solid did not present significant activity changes even after several sequential feed-batch trials and, so that this matter will not be discussed in this paper.

To evaluate the role of the catalyst in the global reaction, new experiments with scavenger agents were performed, adding carbonates to the bulk, so that the reaction efficiency could be compared with the normal process—without any scavenger addition. No abatement on the process efficiency was observed with CO_3^{2-} addition, as shown for TPh removal in Fig. 11, pointing the reaction as mainly driven by surface oxidative reaction rather than by free-radical pathways.

C_{300} was the catalyst selected to be analyzed under scavenging effects for two reasons: (i) it was able to deplete more organic load, being, this way, easier to detect possible efficiency reduction; (ii) it presented the highest iron leaching, and, therefore, more homogeneous reactions were supposed to happen.

Oxidation/reduction potential (ORP) was also followed to evaluate the reaction's capability to oxidize organic matter. The three

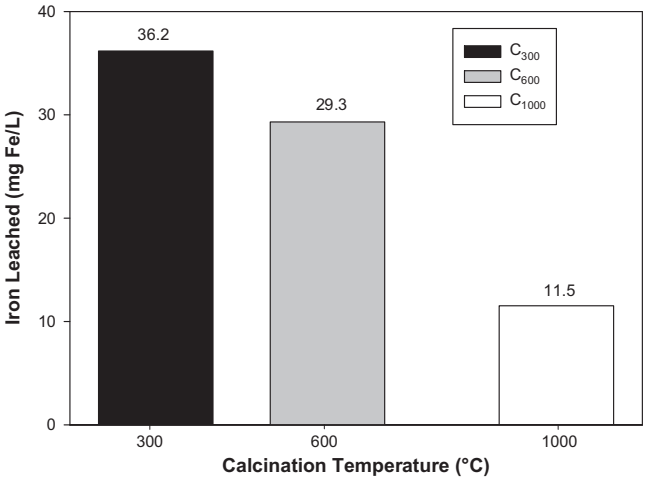

Fig. 10. Amount of iron leached at the end of each catalyst's experiment.

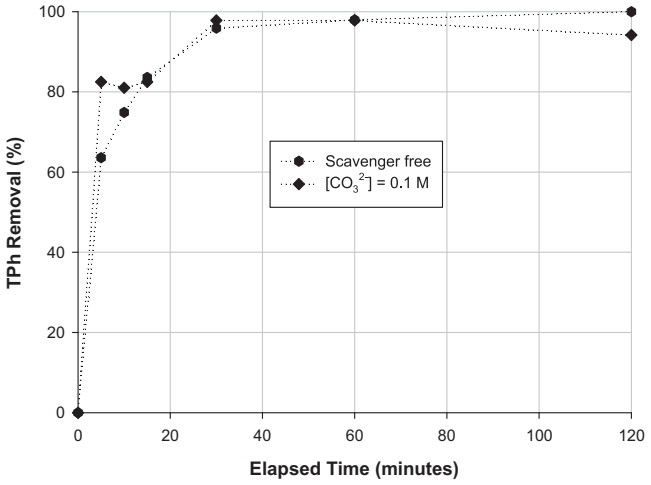

Fig. 11. Total phenolic content removal (%) curves along the heterogeneity comprovement experiments.

catalysts' experiments (Fig. 12a) showed the same values of ORP (measured in the liquid phase), contrarily to the different catalyst behaviours toward COD, TPh and TOC removals, discussed above, revealing that degradation process is indeed mostly undertaken

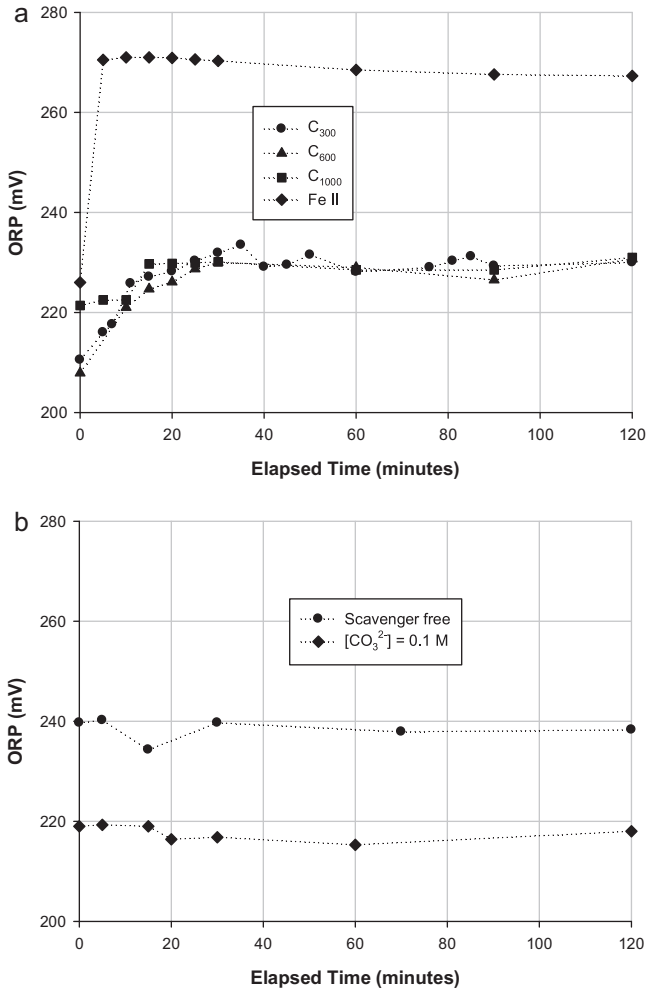

Fig. 12. (a) Oxidation/reduction potential (mV) curves along the experiments for all heterogeneous catalysts. Homogeneous process comparison. (b) Oxidation/reduction potential (mV) curves along the experiments. Scavenger comparison.

in the catalyst surface. This is strengthened when comparing the higher profiles of ORP of the homogeneous process that has its hydroxyl radicals on the bulk. Fig. 12b shows the ORP difference between one experiment containing carbonates as scavenger and the normal reaction for the heterogeneoys C_{300} catalyst. Through its analysis, one can say that there are indeed hydroxyl radicals on the bulk even for the heterogeneous process, although they have no significant contribution in the system efficiency.

4. Conclusions

This work evaluates which is the best calcination temperature of a previously studied catalyst (Fe–Ce–O at the molar proportion of 70/30) facing a synthetic effluent treatment through heterogeneous Fenton's process. 300 °C, 600 °C or 1000 °C were the chosen temperature values. Regarding COD, TOC and TPh removals, C_{300} always presented the best results, followed by C_{600} and, at last, C_{1000}—which was the only catalyst incapable of promoting any TOC removal or to achieve complete phenolic content destruction. C_{1000}, besides providing lesser removals, also presented poor biodegradability enhancement and toxicity depletion. C_{600}, on the other hand, achieved a BOD_5/COD ratio of 0.55 at the end of the reaction, but even this value is not comparable to C_{300}'s: 0.76. C_{300} was then tested in carbonate containing bulk to check if the reaction pathways involved the exit of radicals from the solid's surface to the liquid phase and results indicate that the reaction is, indeed, heterogeneous, taking its place on the solid phase (hypothesis also pointed by ORP examination, which showed a lower potential on the bulk that did not contain carbonate). XRD analysis indicated that the higher the calcination temperature, the higher is the amount of Fe^{3+} on the resulting solid's surface, what might explain the better efficiency of C_{300}—the solid that contains more Fe^{2+}. Also concerning catalyst activity, ORP was followed, but this analysis did not showed significant values between the catalysts. Thus, this potential was not important before taking conclusions about the organic charge removal, reinforcing the fact of the reaction to be taken on the solid's surface.

Acknowledgements

André F. Rossi gratefully acknowledges the Fundação para a Ciência e Tecnologia for the financial support under the PhD grant (SFRH/BD/63653/2009) and also thanks Prof. Dr. Luísa Durães for the acquaintance of analysis results inside the Advanced Materials Characterization subject. Rui C. Martins gratefully acknowledges the Fundação para a Ciência e Tecnologia for the financial support under the Post-Doc grant (SFRH/BPD/72200/2010).

References

[1] F. Haber, J. Weiss, Naturwissenschaften 20 (1932) 948–950.
[2] W.C. Bray, M.H. Gorin, J. Am. Chem. Soc. 54 (1932) 2124.
[3] M. Ahmadi, F. Vahabzadeh, B. Bonakdarpour, E. Mofarrah, M. Mehranian, J. Hazard. Mater. B 123 (2005) 187–195.
[4] P. Cañizares, J. Lobato, R. Paz, M. Rodrigo, C. Sáez, Chemosphere 67 (2007) 832–838.
[5] C. Gomec, R. Erdim, I. Turan, A. Aydin, I. Ozturk, J. Environ. Sci. Health B 42 (2007) 741–747.
[6] M. Kallel, C. Belaid, T. Mechichi, M. Ksibi, B. Elleuch, Chem. Eng. J. 150 (2008) 391–395.
[7] R. Mosteo, P. Ormad, E. Mozas, J. Sarasa, J. Ovelleiro, Water Res. 40 (2006) 1561–1568.
[8] R. Mosteo, J. Sarasa, M. Ormad, J. Ovelleiro, J. Agric. Food Chem. 56 (2008) 7333–7338.
[9] Q. Wang, A.T. Lemley, J. Hazard. Mater. 98 (2003) 241–255.
[10] E. Neyens, J. Baeyens, J. Hazard. Mater. 98 (2003) 33–50.
[11] P. Bautista, A. Mohedano, J. Casas, J. Zazo, J. Rodriguez, J. Chem. Technol. Biotechnol. 83 (2008) 1323–1338.
[12] T. Dantas, V. Mendonça, H. José, A. Rodrigues, R. Moreira, Chem. Eng. J. 118 (2006) 77–82.
[13] S. Shin, H. Yoon, J. Jang, Catal. Commun. 10 (2008) 178–182.
[14] A. Gemeay, I. Mansour, R. El-Sharkawy, A. Zaki, J. Mol. Catal. Chem. 193 (2003) 109.
[15] J.G. Carriazo, E. Guelou, J. Barrault, J.M. Tatibouët, S. Moreno, Appl. Clay Sci. 22 (2003) 303–308.
[16] S. Letaief, B. Casal, P. Aranda, M. Martín-Luengo, E. Ruiz-Hitzky, Appl. Clay Sci. 22 (2003) 263.
[17] I.R. Guimarães, A. Giroto, L.C.A. Oliveira, M.C. Guerreiro, D.Q. Lima, J.D. Fabris, Appl. Catal. B: Environ. 91 (2009) 581–586.
[18] R.C.C. Costa, F.C.C. Moura, J.D. Ardisson, J.D. Fabris, R.M. Lago, Appl. Catal. B: Environ. 91 (2008) 131–139.
[19] R.C. Martins, N. Amaral-Silva, R.M. Quinta-Ferreira, Appl. Catal. B: Environ. 99 (2010) 716–721.
[20] R.G. Lopes, A.M.T. Silva, R.M. Quinta-Ferreira, Appl. Catal. B: Environ. 73 (2007) 193–202.
[21] A.M.T. Silva, I.M. Castelo-Branco, R.M. Quinta-Ferreira, J. Levec, Chem. Eng. Sci. 58 (2003) 963–970.
[22] R.C. Martins, R.M. Quinta-Ferreira, Appl. Catal. B: Environ. 90 (2009) 268–277.
[23] O. Folin, V. Ciocalteu, J. Biol. Chem. LXXIII (1927) 627.
[24] A. Silva, E. Nouli, A. Carmo-Apolinário, N. Xekoukoulakis, D. Mantzavinos, Catal. Today 124 (2007) 232–239.
[25] A. Greenberg, L. Clesceri, A. Eaton, Standard Methods for the Examination of Water and Wastewater, American Public Health Association, Washington, DC, 1985.
[26] R.C. Martins, R. Quinta-Ferreira, Ind. Eng. Chem. Res. 48 (2009) 1196–1202.
[27] J.L. Figueiredo, F. Ramôa Ribeiro, Catálise Heterogênea, Fundação Calouste Gulbenkian.
[28] S. Imamura, M. Nakamura, N. Kawabata, J.I. Yoshida, Ind. Eng. Chem. Prod. Res. Dev. 25 (1986) 34–37.